High contrast all-optical diode based on direction-dependent optical bistability within asymmetric ring cavity*

Xiu-Wen Xia(夏秀文)[1,2,†], Xin-Qin Zhang(张新琴)[1], Jing-Ping Xu(许静平)[2], and Ya-Ping Yang(羊亚平)[2]

[1] School of Mathematics and Physics, Jinggangshan University, Ji'an 343009, China

[2] MOE Key laboratory of Advanced Micro-structure Materials, School of Physics Science and Engineering, Tongji University, Shanghai 200092, China

(Received 1 December 2015; revised manuscript received 18 February 2016; published online 25 June 2016)

We propose a simple all-optical diode which is comprised of an asymmetric ring cavity containing a two-level atomic ensemble. Attributed to spatial symmetry breaking of the ring cavity, direction-dependent optical bistability is obtained in a classical bistable system. Therefore, a giant optical non-reciprocity is generated, which guarantees an all-optical diode with a high contrast up to 22 dB. Furthermore, its application as an all-optical logic AND gate is also discussed.

Keywords: optical diode, optical bistability, optical logic gate

PACS: 42.65.Pc, 42.25.Bs **DOI:** 10.1088/1674-1056/25/8/084211

The optical diode is essential in optical computation and communication,[1–4] as well as in the quantum information processing area. Until now, kinds of non-reciprocal schemes have been fabricated, such as the magneto-optic[5–7] and acousto-optic effects systems,[8] the chiral structures,[9,10] nonlinear parity asymmetric systems,[11–14] etc. However, most of them were either active which need strong external electromagnetic field, or very complicated which need an accurate micro/nano-scale processing technique.

Recently, non-reciprocal light transport has been realized experimentally in a parity-time asymmetric system.[15,16] Parity-time symmetry can be broken by taking into account the gain saturation in an active resonator.[16] Although the coupled active-passive whispering-gallery microcavities can provide a non-reciprocal isolation ratio from -8 dB to $+8$ dB, high-Q resonator is needed and it is not passive. In this work, we will show a high contrast optical diode up to 22 dB in a pure passive system comprised of an asymmetric ring cavity containing a saturable absorptive atomic ensemble, which indicates that active medium, parity-time asymmetry and high-Q resonators are not always necessary.

In our previous work,[17,18] we have shown that the time-reversal asymmetry, spatial asymmetry and optical nonlinearity are three significant factors for optical non-reciprocity, which is consistent with the result of Ref. [19]. In the present work, we will show a giant non-reciprocity in a classical atomic gas-cavity coupling system, which easily fits these three factors. Specifically, optical nonlinearity naturally happens due to saturable absorption of gas, and spatial symmetry can be broken by furnishing different reflectivity walls, meanwhile time-reversal asymmetry is naturally satisfied by taking into account non-radiative dissipations of the cavity and the resonant absorption of atoms.

Although optical absorptive bistability was realized first in 1969,[20] and since then on, a great deal of attention has been paid to observing and understanding the phenomenon of optical bistability[21–24] in symmetric or one-side cavity, there was little work on controllable bistability within asymmetric cavity.[18,25] In our previous work,[18] we have presented a new proposal to obtain giant optical non-reciprocity up to 13 dB by using single-atom controllable bistability in an asymmetric cavity. We have shown that single-atom bistable states were controlled by the asymmetric walls of the cavity and it is feasible to realize the smallest all-optical diode. However, the manipulation of single atom in nano-cavity is still tough in a quantum optical system. It will be much convenient if we can realize this kind of optical diode in a classical optical bistable system.

In this work, we pay attention to the asymmetric ring cavity containing a two-level atomic ensemble which can be performed much more easily under the present technology. More interestingly, we also find an apparent direction-dependent bistability within the asymmetric ring cavity, which can be used to realize a much higher contrast optical diode up to 22 dB. Specifically, under a certain input power, it shall operate in the linear regime ($I_{\rm in} < I_{\rm l}$) for the forward input case while it shall work in the saturated regime ($I_{\rm in} > I_{\rm u}$) for the backward input case. Here $I_{\rm in}$, $I_{\rm l}$, and $I_{\rm u}$ are the input intensity, the lower, and upper threshold intensities of bistability regime, respectively.

The model considered is shown in Fig. 1. This model is similar to the prototype of a Fabry-Perot resonator filled with

*Project supported by the National Natural Science Foundation of China (Grant Nos. 11274242, 11474221, and 11574229), the Joint Fund of the National Natural Science Foundation of China and the China Academy of Engineering Physics (Grant No. U1330203), and the National Key Basic Research Special Foundation of China (Grant Nos. 2011CB922203 and 2013CB632701).

†Corresponding author. E-mail: jgsuxxw@126.com

© 2016 Chinese Physical Society and IOP Publishing Ltd

a saturable absorber presented in Refs. [20] and [26], but it has been modified with asymmetric ring cavity now. To simplify the analysis, its four mirrors M_1, M_2, M_3, and M_4 are lossless. M_3 and M_4 are ideal mirrors with 100% reflectivity, while M_1 and M_2 are different from each other to present the asymmetry of the ring cavity, which are characterized by different reflected and transmitted coefficients, i.e., r_1, r_2, t_1, and t_2, respectively. Meanwhile, their reflectivities and transmittivities are defined by $T_j = |t_j|^2$ and $R_j = |r_j|^2$ $(j = 1, 2)$, respectively. On the upper branch of the ring cavity, it is filled with a saturable two-level atomic ensemble with length l, which is marked by a gray shadow.

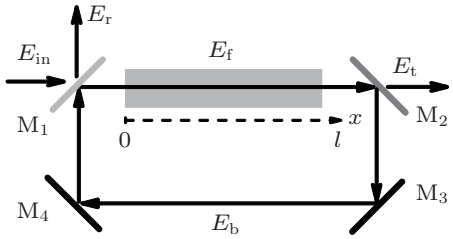


Fig. 1. Schematic diagram of an asymmetric ring resonator. The electric fields E_{in}, E_r, E_t are defined on the mirrors 1 and 2. Arrows show directions of propagation. The gray shadow is the saturable absorber in the cavity with length l.

Here, we distinguish the forward input case from the backward input case. The forward input case is shown in Fig. 1, in which the input field E_{in} is incident from M_1 to M_2, while the backward input case refers to opposite one incident from M_2 to M_1. Taking the forward input case for example, after a similar derivation to that in Ref. [20], we can obtain the relation between input power $I_{in} \propto |E_{in}|^2$ and output power $I_t \propto |E_t|^2$,

$$I_t = I_{in} T_1 T_2 \beta^2 \exp\left[-\int_0^l \alpha(x)\,\mathrm{d}x\right]. \tag{1}$$

where

$$\beta = \left(1 - r_1 r_2 \exp\left(-\int_0^l \alpha(x)\,\mathrm{d}x/2\right)\right)^{-1}$$

refers to the multi-reflection in cavity. Unlike the usual linear optics, the absorption coefficient $\alpha(x)$ is dependent on the field intensity in the saturable two-level atomic ensemble $I_f \propto |E_f|^2$ and it is also position-dependent in general, which can be expressed as

$$\alpha(x) = \alpha_0/[1 + I_f(x)/I_s] \quad (0 < x < l). \tag{2}$$

Here, α_0 is the linear absorption coefficient and I_s is the critical power of saturable atomic ensemble. The field intensity in the saturable medium I_f is also related to nonlinear absorption coefficient, writing

$$I_f(x) = I_t \exp\left[\int_0^x \alpha(x')\,\mathrm{d}x'\right]/T_2. \tag{3}$$

By using the iterative method we can solve Eqs. (1)–(3) numerically and obtain the steady relationship between I_t and I_{in}. The method adapted here is a little different from the mean field approximation adopted in Refs. [20] and [26] concerning the optical bistability in symmetry cavity, in which the nonlinear absorption coefficient α was spatially averaged and independent of its position. It should be pointed out that for the backward input case, equations (1) and (2) are not changed, but T_2 should be replaced by T_1 in Eq. (3).

In order to check the availability of our method, we calculate the input-output relation for the case of symmetric cavity first, i.e., $R_1 = R_2$. By fixing the linear absorption coefficient as $\alpha_0 l = 3.75$ which was presented in Ref. [20], the curves of I_t versus I_{in} are plotted in Fig. 2(a) with different values of $R_1 = R_2$. The figure shows that when $R_1 = R_2 > 0.8$, the optical bistability happens. For any bistable state, bistable regime is characterized by two threshold intensities I_l and I_u. On the other hand, by fixing the mirrors of $R_1 = R_2 = 0.9$, we plot the curves of I_t versus I_{in} in Fig. 2(b) with different values of $\alpha_0 l$. It shows that the bistable states happen when $\alpha_0 l > 1.25$. These results are in accordance with the results in previous studies and show that the bistable states appear only in a definite range of input intensities with using appropriate parameters.[21]

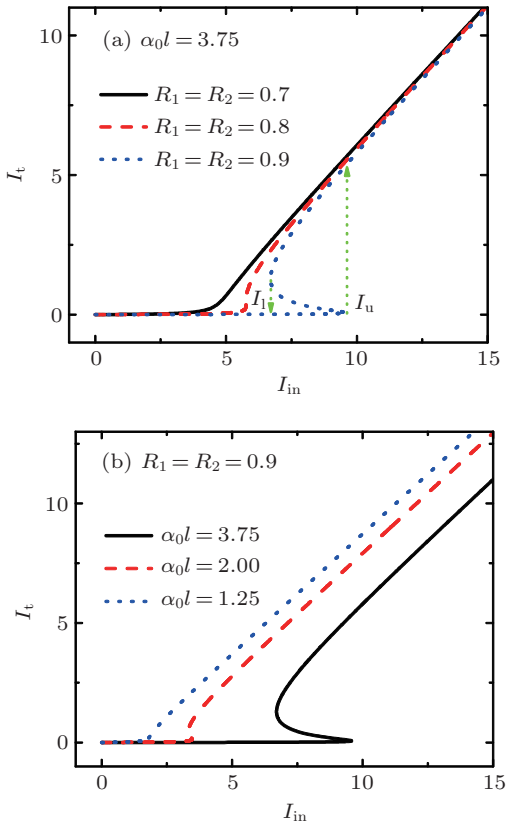


Fig. 2. (color online) Optical bistability in symmetric ring cavity. In panel (a) we take $\alpha_0 l = 3.75$, and $R_1 = R_2 = 0.7$, 0.8, 0.9, and the bistable state of $R_1 = R_2 = 0.9$ taken for example, optical bistable regime (I_l, I_u) bounded by two green dotted lines, which separate it from the linear regime $(0, I_l)$ and saturated regime (I_u, ∞). In panel (b) we set $R_1 = R_2 = 0.9$ and $\alpha_0 l = 1.25$, 2.00, and 3.75.

Now we discuss the direction-dependent optical bistability induced by spatial symmetry breaking in the asymmetric ring cavity. The reflectivities of mirrors M_1 and M_2 are set to be $R_1 = 0.8$ and $R_2 = 0.9$ to present asymmetric ring cavity, respectively. By fixing $\alpha_0 l = 3.75$, the relations between I_t and I_{in} for forward and backward input cases are plotted as the solid and dashed curves in Fig. 3(a), respectively. Comparing the curves in Fig. 3(a) with the blue and red curves in Fig. 2(a), we find that bistable phenomena in the asymmetric cavity are very different from those in the symmetric cavity. In a spatial asymmetric system, optical bistability is direction-dependent now.

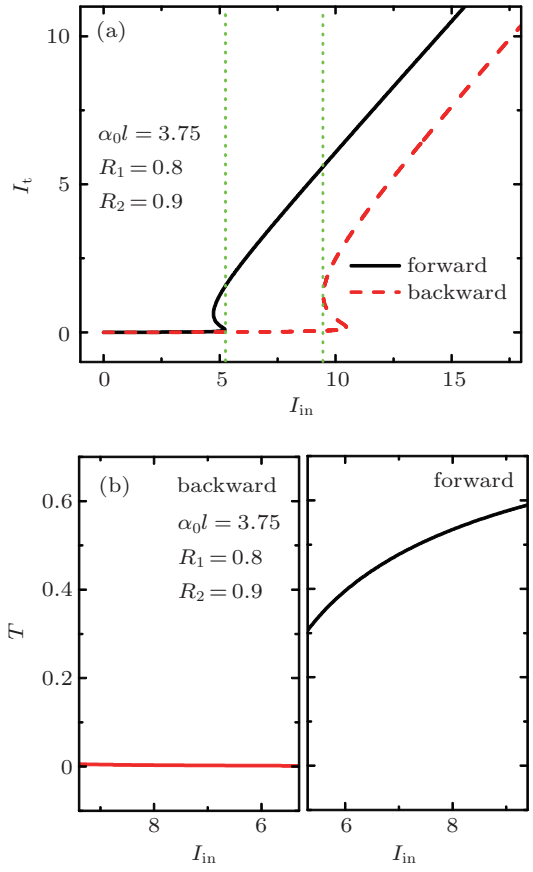


Fig. 3. (color online) Direction-dependent optical bistability and non-reciprocity in asymmetric ring cavity. We take $\alpha_0 l = 3.75$, and $R_1 = 0.8$, $R_2 = 0.9$ to present the asymmetry of the cavity. Panel (a) shows the I_t versus I_{in}, where the black solid line refers to the forward input case and red dashed line to the backward input case. The two vertical green dotted lines indicate the optimal input intensity window. Panel (b) shows T versus I_{in} in the optimal window, where the black line denotes the forward transmittivity T_f and the red curve represents the backward transmittivity T_b.

For the forward input case, input field is incident on M_1 with $R_1 = 0.8$ at first, and the solid curve in Fig. 3(a) is similar to the red dashed curve in Fig. 2(a), but the bistable regime of I_{in} in asymmetric cavity is much wider than that in symmetric cavity with $R_1 = R_2 = 0.8$. For the backward input case, the input field is incident on M_2 with $R_2 = 0.9$ at first, and the dashed curve in Fig. 3(a) is more similar to the blue dotted curve in Fig. 2(a), but the bistable regime for backward input case is narrower than that of symmetric cavity with $R_1 = R_2 = 0.9$. Therefore, in the asymmetric cavity, optical bistability is highly direction-dependent. The result of direction-dependent absorptive bistability in classical system is in line with our previous prediction of controllable single atom bistability in quantum optical system.[18]

The non-reciprocal transport in the present asymmetric system originates from the varying optical nonlinearities induced by absorption saturation in two input cases, which is similar to that in the active system.[16] More importantly, our scheme works in the bistable regime while the active system does not, which is the reason why our scheme can generate much higher transmission contrast than previous ones. In this work, the optical bistable regime is separated significantly between the forward and backward input cases. Therefore, our scheme will provide excellent optical non-reciprocity. Furthermore, our scheme is passive and without high-Q resonators.

Here, we show how to construct an efficient optical diode under the optimal window of operation power. As shown in Fig. 3(a), when the input power is located in the optimal window, i.e., $I_{in} \in [5.24, 9.48]$, forward input field can transport the cavity easily but the backward input field is blocked completely. The values of normalized transmittivity $T = I_t/I_{in}$ for the forward input case T_f and backward input case T_b are plotted in Fig. 3(b) in the optimal window. It is shown that the optical diode contrast $C = 10 \times \log_{10}(T_f/T_b)$ can easily reach 22 dB in the present classical optical bistable system.

To explain such a direction-dependent optical bistability and non-reciprocity analytically, we explore the bistability condition in detail. Since the value of αl is near zero undergoing large input power, the exponential term $e^{-\alpha l}$ can be approximated by $1 - \alpha l$. Taking the forward input case for example, with the definition of $X = I_{in}/(I_s T_2)$ and $Y = I_t/(I_s T_2)$, the equation connecting the input power I_{in} and the transmitted power I_t can be simplified into

$$X = Y\left(p + \frac{k_0}{1+Y}\right)^2, \tag{4}$$

where $p = (1 - r_1 r_2)/(t_1 t_2)$ and $k_0 = \alpha_0 l \cdot r_1 r_2/(2 t_1 t_2)$. If Y has three solutions for a certain X, then bistability happens. The thresholds of bistability for Eq. (4) are the solutions of equation $B^2 - 4AC = 0$, where $A = b^2 - 3ac$, $B = bc - 9ad$, $C = c^2 - 3bd$, and $a = p^2$, $b = 2p(p + k_0) - X$, $c = (p + k_0)^2 - 2X$, $d = -X$. Notice that equation (4) is independent of the input direction because r_1 and r_2 as well as t_1 and t_2 always appear in couples, therefore the threshold of X for bistability is direction-independent.

However, the threshold intensities I_l and I_u are direction-dependent due to the definition $X = I_{in}/(I_s T_2)$. For the case of forward input, I_l (I_u) $\propto T_2$. Meanwhile for the case of backward input, I_l (I_u) $\propto T_1$. In Fig. 3, $T_1 = 0.2$ and $T_2 = 0.1$, the threshold I_l and I_u for the forward input case (solid curve)

are 4.74 and 5.12, respectively; meanwhile I_l and I_u for the backward input case (dashed curve) are 9.48 and 10.24, respectively, which are double compared with the threshold intensities in the forward input case. It presents a remarkable direction-dependent bistability in the asymmetric cavity.

The direction-dependent optical bistability can be used not only as optical diode or isolator, but also as optical switching, memory, transistor,[27] etc. Here we introduce a new application as optical logic AND gate. Despite the superiority of such a kind of logic gate, our proposal provides a new access to it at least. The block diagram of such a logic AND gate is shown in Fig. 4, where two optical signals I_a and I_b are incident on the left wall M_1 of saturated bistable optical device through an add/drop filter and output signal I_t transports from the right wall M_2. We present a random phase mask on the line of I_b to ensure the two input fields are fully decoherent. Therefore, the input power is $I_{in} = I_a + I_b$. After transmitting through the saturable absorptive bistable device, the output power I_t depends on the optical bistable state.

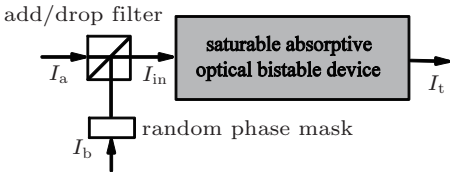


Fig. 4. Block diagram of an all-optical AND gate.

Here, optical logic states 0 and 1 are characterized by the intensity of the field, which can be defined as

$$\text{bit} = \begin{cases} 0, & I \in [0, \delta_e], \\ 1, & I \in [I_1 - \delta_e, I_1 + \delta_e], \end{cases} \tag{5}$$

where I_1 and δ_e ($\ll I_1$) are the threshold intensity of logic 1 and its tolerance, respectively. In order to obtain logic AND gate, $I_{in} = I_1$ should be located in the linear regime while $I_{in} = 2I_1$ in the saturated regime with $I_t(2I_1) = I_1$ to ensure the output logic state is true.

As is well known, the output power I_t in the saturated regime can be simplified into a linear function, i.e., $I_t = a + b \cdot (I_{in} - I_l)$, where a and b are the fitting parameters. In principle, a and b as well as I_l can be adjusted by the reflectivities of walls. Logic AND gate should fulfill the following conditions at least, i.e. $\delta_e < a/2$ and $I_1 \in (I_u/2 + a/2, I_l - a/2)$.

As an example, we set $\alpha_0 l = 3.75$, $R_1 = 0.8$, $R_2 = 0.9$ and plot curve of I_t versus I_{in} in Fig. 5 to illustrate the operating power of optical AND gate. After numerical simulation and linear fitting we obtain $I_l = 4.74$, $I_u = 5.24$, $a = 1.07$, and $b = 1.017$. Therefore, with the coded power $I_1 = 3.69$ and $\delta_e < 0.51$, we can realize the optical logic AND gate. It can be easily verified that only for logic input state (1,1) the output logic state is true when we calculate the output I_t at different input states as shown in Table 1. It should be pointed out that although we take an asymmetric system for example here to illustrate logic AND gate, it is different from such a kind of optical diode. To construct such a kind of logic AND gate, the spatial asymmetry is not always necessary.

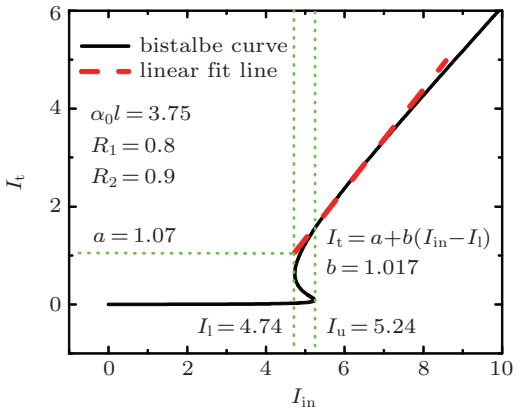


Fig. 5. (color online) Illustration of optical logic AND gate. We set $\alpha_0 l = 3.75$, $R_1 = 0.8$, and $R_2 = 0.9$, the linear fit curve in the saturated regime is plotted as a red dashed line. We can obtain the values of I_l, I_u, and a to be 4.74, 5.24, and 1.07 from the bistable curve, respectively. The two vertical green dotted lines characterize the bistable regime $I_u - I_l$ and the horizontal green dotted line shows the value of a.

Table 1. Logical operations of AND gate.

I_a	I_b	Input logic state	I_t	Output logic state
0	0	(0,0)	0.00	0
0	3.69	(0,1)	0.01	0
3.69	0	(1,0)	0.01	0
3.69	3.69	(1,1)	3.69	1

Finally, we discuss the experimental proposal to such an optical diode and a logic AND gate. Since there are many bistable experiments done in symmetric classical macro cavity, we can retain their main equipment presented in Ref. [20] but only replace the symmetric cavity with the asymmetric ring cavity. However, the bistable operating power was rather high in the past work and it should be lowered to an acceptable level. As is well known, the saturable critical power $I_s \propto 1/\mu^2\tau$,[20,28,29] where μ and τ are atomic dipole moment and the atomic lifetime of the saturable medium in the resonator, respectively. Thus larger μ and τ are beneficial to lower I_s.[22] Recently, there were a remarkable series of experiments in bistable multiple-quantum-well devices that lowered the critical power to an acceptable level.[24,27] Since silicon-based optical micro devices are desired, we also present a possible experimental proposal based on micro/nano technology. Recently, on-chip whispering-gallery microcavities with gain and loss have been fabricated.[16] Therefore, it is not difficult to construct such a four-mirror ring cavity with loss in one of the rectangle sides after careful designing. Four Bragg reflectors[30] should be placed in the corners of ring cavity and the spatial asymmetry can be obtained by furnishing different

Bragg reflectors. Therefore, it is feasible to realize such a kind of optical diode and logic AND gate.

References

[1] Wang D W, Zhou H T, Guo M J, Zhang J X, Evers J and Zhu S Y 2013 *Phys. Rev. Lett.* **110** 093901

[2] Fan L, Wang J, Varghese L T, Shen H, Niu B, Xuan Y, Weiner A M and Qi M 2012 *Science* **335** 447

[3] Wang C, Zhong X L and Li Z-Y 2012 *Sci. Rep.* **2** 674

[4] Hu X, Li Z, Zhang J, Yang H, Gong Q and Zhang X 2011 *Adv. Funct. Mater.* **21** 1803

[5] Espinola R L, Izuhara T, Tsai M C, Osgood J R M and Dötsch H 2004 *Opt. Lett.* **29** 941

[6] Zaman T R, Guo X and Ram R J 2007 *Appl. Phys. Lett.* **90** 023514

[7] Bi L, Hu J, Jiang P, Kim D H, Dionne G F, Kimerling L C and Ross C A 2011 *Nat. Photon.* **5** 758

[8] Ibrahim S K, Bhandare S, Sandel D, Zhang H and Noe R 2004 *Electron. Lett.* **40** 1293

[9] Fedotov V A, Mladyonov P L, Prosvirnin S L, Rogacheva A V, Chen Y and Zheludev N I 2006 *Phys. Rev. Lett.* **97** 167401

[10] Allahverdyan K R, Gevorgyan A H, Hakobyan R S and Galstian T V 2013 *JETP Lett.* **96** 694

[11] Zheng J, Fang Y, Hu J and Yang L 2014 *J. Nanoelectron. Opt.* **9** 406

[12] Shen H Z, Zhou Y H and Yi X X 2014 *Phys. Rev. A* **90** 023849

[13] Bulgakov E N and Sadreev A F 2014 *Opt. Lett.* **39** 1787

[14] Gallo K and Assanto G 1999 *J. Opt. Soc. Am. B* **16** 267

[15] Peng B, Ozdemir S K, Lei F, Monifi F, Gianfreda M, Long G L, Fan S, Nori F, Bender C M and Yang L 2014 *Nat. Phys.* **10** 394

[16] Chang L, Jiang X, Hua S, Yang C, Wen J, Jiang L, Li G, Wang G and Xiao M 2014 *Nat. Photon.* **8** 524

[17] Xia X W, Xu J P and Yang Y P 2014 *J. Opt. Soc. Am. B* **31** 2175

[18] Xia X W, Xu J P and Yang Y P 2014 *Phys. Rev. A* **90** 043857

[19] Jalas D, Petrov A, Eich M, Freude W, Fan S, Yu Z, Baets R, Popovic M, Melloni A, Joannopoulos J D, Vanwolleghem M, Doerr C R and Renner H 2013 *Nat. Photon.* **7** 579

[20] Szoke A, Daneu V, Goldhar J and Kurnit N 1969 *Appl. Phys. Lett.* **15** 376

[21] Joshi A, Brown A, Wang H and Xiao M 2003 *Phys. Rev. A* **67** 041801

[22] Prataviera G A, Yoshida A C and Mizrahi S S 2013 *Phys. Rev. A* **87** 043831

[23] Bonifacio R and Lugiato L A 1978 *Phys. Rev. Lett.* **40** 1023

[24] Pellegrini V, Fuso F, Arimondo E, Castelli F, Lugiato L, Bava G and Debernardi P 1994 *Phys. Rev. A* **50** 5219

[25] Mitchell N, Connolly J, O'Gorman J and Hegarty J 1994 *Opt. Lett.* **19** 269

[26] Bonifacio R and Lugiato L A 1978 *Phys. Rev. A* **18** 1129

[27] Ballarini D, De Giorgi M, Cancellieri E, Houdré R, Giacobino E, Cingolani R, Bramati A, Gigli G and Sanvitto D 2013 *Nat. Commun.* **4** 1778

[28] Rosenberger A T, Orozco L A, Kimble H J and Drummond P D 1991 *Phys. Rev. A* **43** 6284

[29] Shakhmuratov R N, Odeurs J and Mandel P 2007 *Phys. Rev. A* **75** 013808

[30] Yüce E, Ctistis G, Claudon J, Dupuy E, Buijs R D, de Ronde B, Mosk A P, Géard J M and Vos W L 2013 *Opt. Lett.* **38** 374